*Progress In Electromagnetics Research Letters, Vol. 56, 81–87, 2015*

# Decoupled Hepta-Band Antenna Array with Three Slots for WWAN/LTE Mobile Terminals

**Hui-Fen Huang*** **and Ting Li**

**Abstract**—A hepta-band covering GSM850/900/1800/1900/UMTS/LTE2300/LTE2500 handset antenna array is presented. The antenna array consists of two symmetric antenna elements, a T-shaped protruded ground (TP) and three slots. The antenna element consists of a feed strip and two radiation strips (RS1, RS2), which only occupies a planar size of $15 \times 25\,\text{mm}^2$ and generates dual-mode resonances at $\lambda/8$ and $\lambda/4$. The three slots and T-shaped protruded ground are utilized to reduce mutual coupling. Different slots can adjust different frequency bands independently. The working mechanism of the three slots is analyzed based on $S$-parameters and surface current distributions. The measured $S_{11}$ and $S_{12}$ are lower than $-6\,\text{dB}$ and $-15\,\text{dB}$ in the working bands, respectively. The radiation patterns and diversity performance are presented.

## 1. INTRODUCTION

Nowadays, with the great development of wireless communication, the demand for high quality and high data rate transmission is increasing. It has been demonstrated that multiple-input-multiple-output (MIMO) is a promising technology to achieve this target. The MIMO technology can improve the communication quality and increase the system capacity by using multiple antennas at the transmitter and receiver [1]. It has already been widely used in the base station antenna. However, there still exist the following challenges: (1) The conflicting considerations of multifunction and miniaturization lead to a continuous challenge in mobile handset antenna design. (2) As the no-ground space left for antenna is small in the mobile terminal, the mutual coupling between the antennas is strong, which makes it difficult to design a MIMO antenna applied in the mobile terminal. Several methods have been proposed to reduce the antenna size, mainly including coupled-feed [2], double-side structure [3], loading lumped chip elements [4] and 3-D structure [5]. Many works have been done for decoupling. Three neutralization lines were used to achieve low mutual coupling in a wide bandwidth, covering 1710–2690 MHz in [6]. Two antenna elements share a common radiator in [7]. High isolation between the two antenna elements is achieved by etching a T-shaped slot in the radiator and extending a stub on the ground. Parasitic element was studied for UMTS band [8]. Lumped chip elements are loaded in [9]. Some other methods were also used to reduce mutual coupling, including decoupling network [10], defected ground structure [11] and polarization decoupling method [12]. In [13, 14], a slot is included to improve the isolation in the 824–960 MHz bands and shows the impact on the multiplex efficiency. In the near future, the 2G/3G/4G communication systems will coexist for a long time. It is promising to design a MIMO antenna, which covers the GSM850/900/1800/1900, UMTS, LTE2300, and LTE2500 for 2G/3G/4G communications. More recently, low-frequency MIMO antenna systems for GSM850/900/DCS/PCS/UMTS/LTE2500 and GSM 900/1800/1900/UMTS were proposed in [15], respectively.

*Received 20 July 2015, Accepted 8 September 2015, Scheduled 22 September 2015*

* Corresponding author: Hui-Fen Huang (jia.luyang@mail.scut.edu.cn).

The authors are with the School of Electronic and Information Engineering, South China University of Technology, Guangzhou, China.

In this paper, a hepta-band covering GSM850/GSM900 (824–960 MHz), GSM1800/GSM1900/UMTS /LTE2300/LTE2500 (1710–2690 MHz) handset antenna is achieved in a ground plane 110 mm × 70 mm × 0.8 mm FR4 printed on an FR4 substrate. The developed hepta-band antenna has smaller size and better isolation than published literatures [6, 9]. The following technique is used to reduce the size: The antenna element is fed by a microstrip line through capacitive coupling, and then dual-mode resonances are excited at $\lambda/8$ and $\lambda/4$. Three etched slots and a T-shaped protruded ground in the ground plane are used to reduce the coupling between two antenna elements. In the mean time, different bands can be adjusted independently by three slots respectively. The measured $S_{11}$ and $S_{12}$ are lower than −6 dB, and −15 dB in the working bands, respectively. The antenna description and analysis is in Section 2. Experimental results are presented in Section 3. Conclusion is in Section 4.

## 2. ANTENNA DESCRIPTION AND ANALYSIS

Figure 1(a) is the geometry of the proposed antenna with antenna element size 15 × 25 mm$^2$. The proposed dual-antenna is printed on a 110 × 70 × 0.8 mm FR4 substrate with relative permittivity 4.4 and loss tangent 0.02. The MIMO antenna consists of two symmetric antenna elements, ground plane and micro-strip feeding line. Each antenna element consists of two radiation strips (RS1 and RS2). RS1 and the 50 Ohm microstrip feeding line are on one side of the substrate, and RS2 and the ground plane are on the other side. The antenna element is fed by a microstrip line through capacitive coupling, and then dual-mode resonances are excited at $\lambda/8$ and $\lambda/4$. Three etched slots and a T-shaped protruded ground in the ground plane are used to reduce the coupling between two antenna elements. Strip RS1 (as in Fig. 1(b)) contributes to 850 and 1850 MHz modes, and strip RS2 (as in Fig. 1(c)) contributes to 925 and 2200 MHz modes. The four resonance modes cover the whole working bands.

Figure 2(a) shows the constructing process of the decoupling structure. Ant1 has no decoupling structure; Ant2 has T-shaped decoupling structure; Ant3 has three slots decoupling structure; the proposed antenna has both T-shaped protruded ground and three slots. The simulated $S_{11}$ and $S_{12}$ for Ant1–3 and the proposed antenna are shown in Figs. 2(b), (c), respectively. It can be observed that without the decoupling structure, $S_{12}$ is higher than −10 dB in both low and high frequency bands, which is considered as poor isolation in the case of a mobile terminal. The slots and T-shaped protruded ground greatly reduce the coupling between two antennas from −6 dB to less than −15 dB. The T-shaped protruded ground is treated as a reflector of electromagnetic wave, which separates the

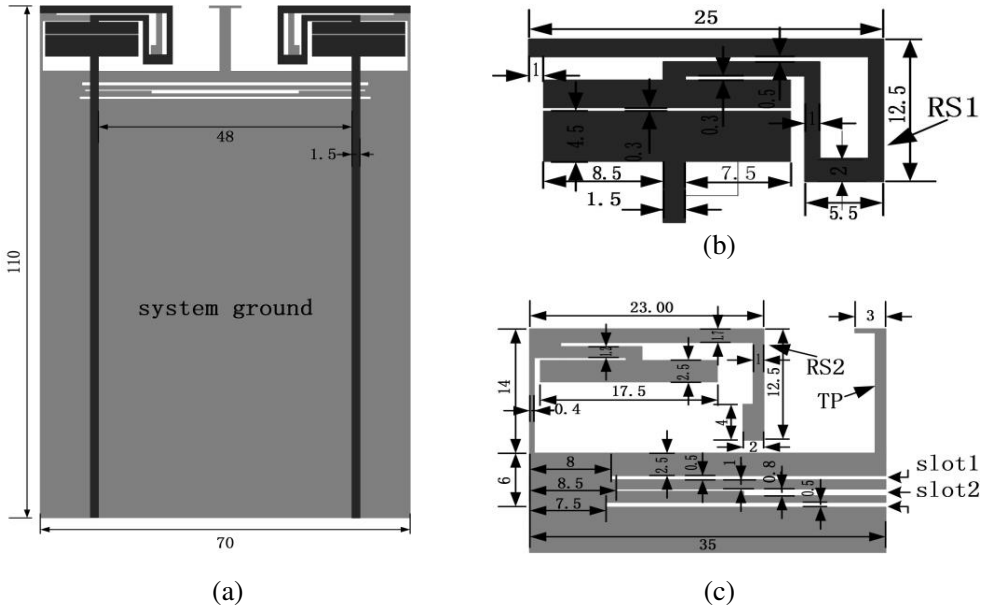


**Figure 1.** The geometry of the (a) proposed antenna, (b) front-side, (c) back-side.

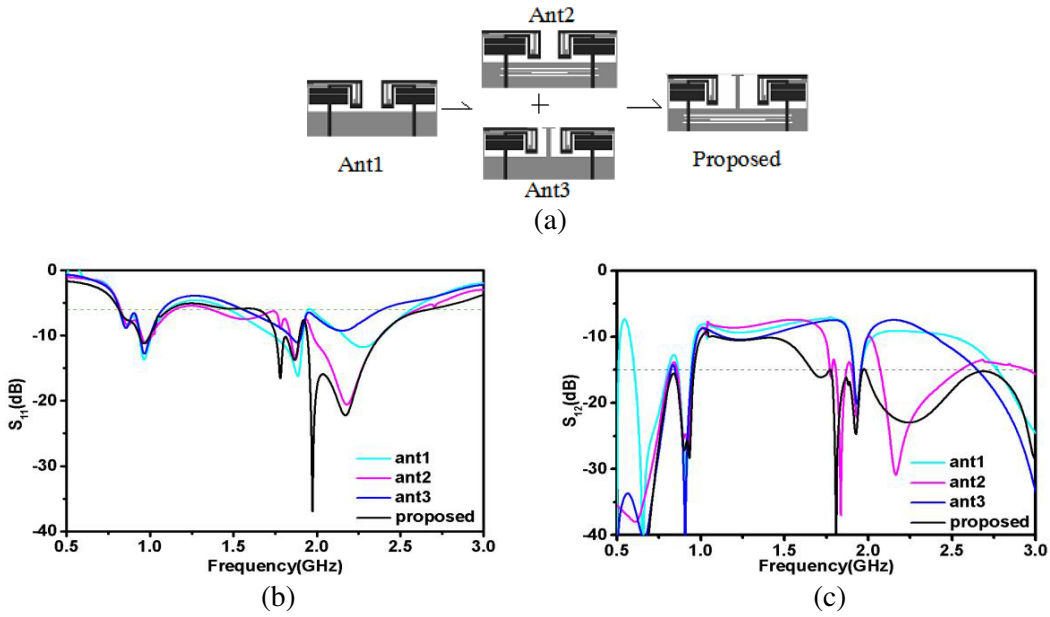


**Figure 2.** Decoupling structure analysis: (a) Constructing process, (b) $S_{11}$, and (c) $S_{12}$.

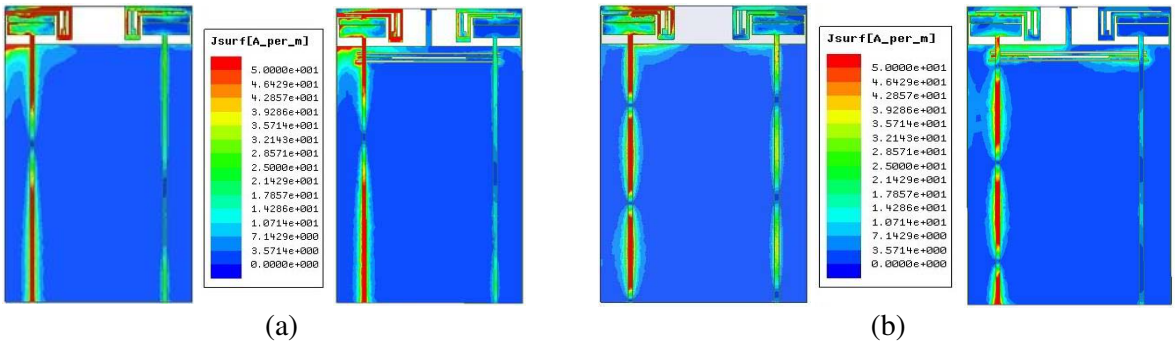


**Figure 3.** Simulated surface current distributions without (left) and with (right) the three slots at (a) 0.85 GHz, (b) 2.25 GHz.

radiation patterns of the two antennas. The slot antennas produce new current in the ground to offset the original current produced by the two antenna elements.

To explain this further, the simulated surface current distributions on antenna with and without the decoupling structure at 850 MHz and 2.5 GHz are shown in Figs. 3(a) and (b), respectively. The current distribution in Fig. 3 is obtained under the condition that port 1 is excited while port 2 is terminated to a matching load. It can be seen that the current flowing into port 2 is significantly reduced by introducing the decoupling structure compared to the current flowing into port 2 when there is no decoupling structure between the two antenna elements of the MIMO configuration.

$S_{11}$ and $S_{12}$ for antenna with one of the three slots and T-shaped protruded ground (TP) are shown in Figs. 4(a) and (b), respectively. Different slots correspond to different resonance points, and the performance in different operation bands can be adjusted independently by slot1, slot2 and slot3, respectively.

## 3. EXPERIMENTAL RESULTS

The developed antenna is fabricated as shown in Fig. 5. The simulated and measured $S_{11}$ and $S_{12}$ for the proposed MIMO antenna are shown in Fig. 6, and the measured and simulated results agree well. In

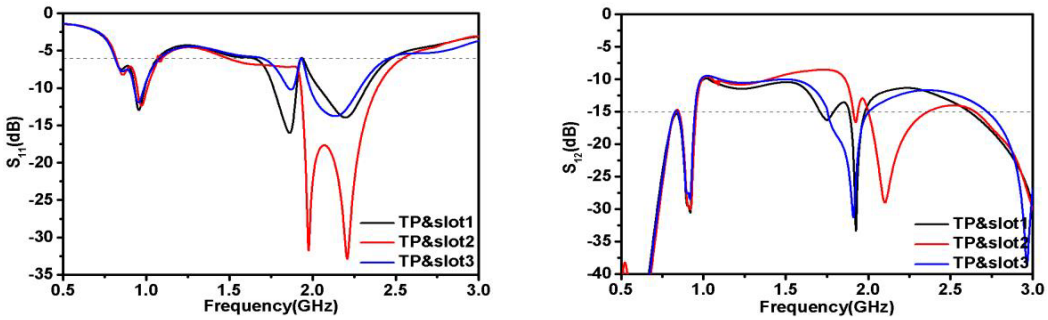


**Figure 4.** $S$-parameter with only one slot and TP. (a) $S_{11}$, (b) $S_{12}$.

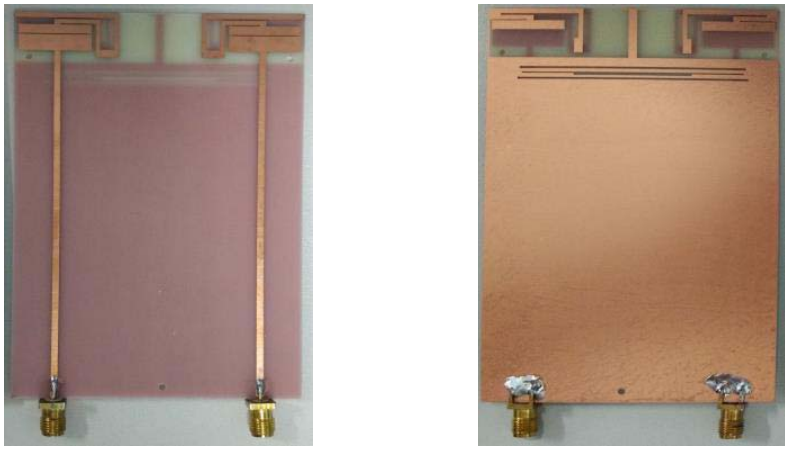


**Figure 5.** Prototype of the proposed dual-antenna: (a) Bottom side, (b) top side.

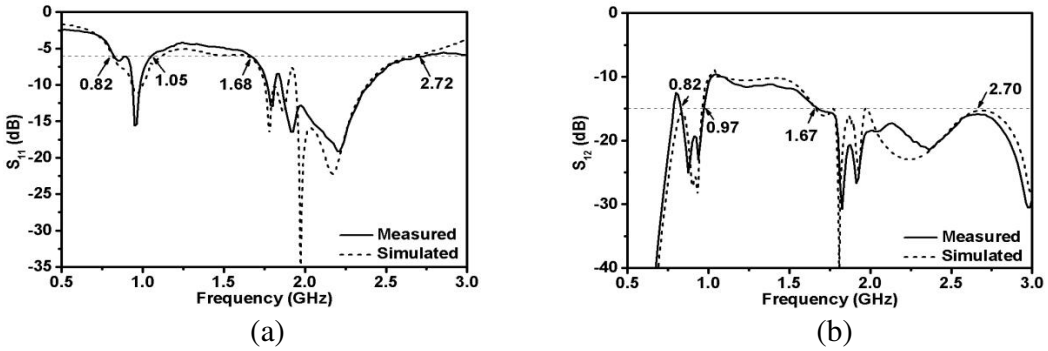


**Figure 6.** Simulated and measured $S$-parameters of the proposed antenna. $S_{11}$, (b) $S_{12}$.

the operation band (824–960 MHz and 1710–2690 MHz), $S_{11}$ and $S_{12}$ are lower than $-6$ dB and $-15$ dB, respectively.

Figure 7 shows the measured radiation patterns in the $xy$-plane, $xz$-plane, and $yz$-plane at 0.85 GHz, 1.9 GHz and 2.4 GHz. It is obvious that the radiation patterns of the two antenna elements have good complementation in the space. This property provides good antenna diversity in a rich scattering environment. Fig. 8 shows the measured gain and efficiency of the proposed dual-antenna.

To evaluate the diversity performances of the proposed dual-antenna, Table 1 shows the envelope

correlation coefficients ($\rho$e12), mean effective gains (MEG), and diversity gain (DG). $\rho$e12 and MEG are calculated using the measured result with the approach in [16]. Parameter $\Gamma$ is the cross-polarization discrimination (XPD) (ratio of vertical to horizontal power density) of the incident field. $\Gamma$ is 0 and 6 dB. From the table, it can be seen that the proposed antenna can meet the demands of $|\text{MEG1}-\text{MEG2}| < 3$ dB and $\rho\text{e12} < 0.5$ over all the desired bands, which indicates that it suits the criteria of comparable average received power and low correlation.

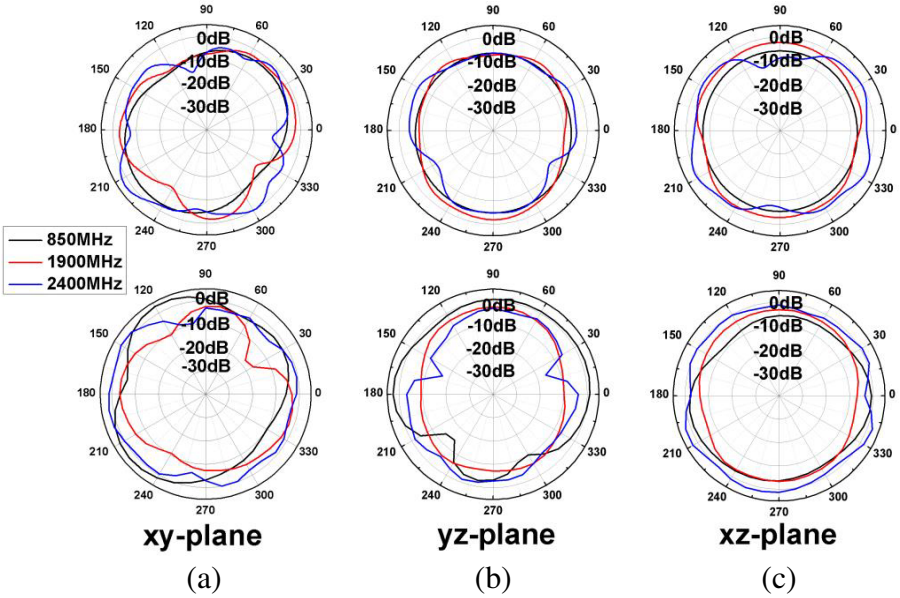


**Figure 7.** Measured radiation patterns for antenna elements-1(up), elements-2(down) at different frequencies.

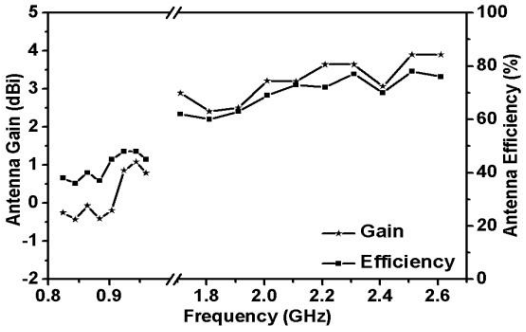


**Figure 8.** Measured antenna gain and efficiency of the proposed antenna.

**Table 1.** Diversity performance of the proposed dual-antenna.

| Frequency (GHz) | $\Gamma$ (dB) | MEG1 (dBi) | MEG2 (dBi) | $\rho$e12 | Diversity gain (1%) (dB) |
|---|---|---|---|---|---|
| 0.85 | 0 | −7.60 | −7.85 | 0.006 | 9.73 |
| | 6 | −8.89 | −9.15 | | |
| 1.9 | 0 | −7.47 | −7.07 | 0.067 | 9.44 |
| | 6 | −7.49 | −7.14 | | |
| 2.4 | 0 | −5.08 | −5.57 | 0.043 | 9.41 |
| | 6 | −5.43 | −5.84 | | |

## 4. CONCLUSION

A compact and multiband MIMO antenna system covering GSM850/900/1800/1900/UMTS/LTE2300/LTE2500 is developed in this letter. The MIMO antenna system consists of two symmetric antenna elements and a decoupling structure. The capacitive coupling feed is used to generate $\lambda/8$ and $\lambda/4$ resonance mode to reduce the size. Both simulation and measurement show good results. The achieved isolation is less than $-15$ dB in the working band. The radiation patterns are measured and cover complementary spatial regions. The envelope correlation coefficients are evaluated.

## ACKNOWLEDGMENT

This work is supported by the National Natural Science Foundation of China under Grant 61071056. Characteristics of Innovation Foundation of Department of Education of Guangdong Province 2014KTSCX017.

## REFERENCES

1. Jensen, M. A. and J. W. Wallace, "A review of antennas and propagation for MIMO wireless communication," *IEEE Trans. Antennas Propag.*, Vol. 52, No. 11, 2810–2824, Nov. 2004.
2. Chang, C. H. and K. L. Wong, "Printed $\lambda/8$-PIFA for penta-band WWAN operation in the mobile phone," *IEEE Trans. Antennas Propag.*, Vol. 57, No. 5, 1373–1381, May 2009.
3. Zhang, T., R. L. Li, G. P. Jin, G. Wei, and M. M. Tentzeris, "A novel multiband plannar antenna for GSM/UMTS/LTE/Zigbee/RFID mobile device," *IEEE Trans. Antennas Propag.*, Vol. 59, No. 11, 4209–4214, Nov. 2011.
4. Wong, K. L. and C. T. Lee, "Wideband surface-mount chip antenna for eight-band LTE/WWAN slim mobile phone application," *Microwave and Optical Technology Letters*, Vol. 52, No. 11, 2554–2560, Nov. 2010.
5. Guo, Q. X., R. Mittra, F. Lei, Z. R. Li, J. L. Ju, and J. Byun, "Interaction between internal antenna and external antenna of mobile phone and hand effect," *IEEE Trans. Antennas Propag.*, Vol. 61, No. 2, 862–870, Feb. 2013.
6. Wang, Y. and Z. W. Du, "A wideband printed dual-antenna with three neutralization lines for mobile terminals," *IEEE Trans. Antennas Propag.*, Vol. 62, No. 3, 1495–1500, Mar. 2014.
7. Mao, C. X. and Q. X. Chu, "Compact coradiator UWB-MIMO antenna with dual polarization," *IEEE Trans. Antennas Propag.*, Vol. 62, No. 9, 4474–4480, Feb. 2014.
8. Li, Z., Z. Du, M. Takahashi, K. Saito, et al., "Reducing mutual coupling of MIMO antennas with parasitic elements for mobile terminals," *IEEE Trans. Antennas Propag.*, Vol. 60, No. 2, 473–481, Feb. 2012.
9. Ban, Y.-L., Z.-X. Chen, et al., "Decoupled closely spaced hepta-band antenna array for WWAN/LTE smart phone applications," *IEEE Antennas Wireless Propag. Letts*, Vol. 13, 31–34, 2014.
10. Chen, S.-C., Y.-S. Wang, and S. J. Chung, "A decoupling technique for increasing the port isolation between two strongly coupled antennas," *IEEE Trans. Antennas Propag.*, Vol. 56, No. 12, 3650–3658, Dec. 2008.
11. Chiu, C.-Y., C.-H. Cheng, R. D. Murch, et al., "Reduction of mutual coupling between closely-packed antenna elements," *IEEE Trans. Antennas Propag.*, Vol. 55, No. 6, 1732–1738, Jun. 2007.
12. Li, Y., et al., "Design of dual-polarized monopole-slot antenna with small volume and high isolation," *IEEE Trans. Antennas Propag.*, Vol. 60, No. 5, 2511–2514, May 2012.
13. Andújar, A. and J. Anguera, "MIMO multiband antenna system combining resonant and non-resonant elements," *Microwave and Optical Technology Letters*, Vol. 56, No. 5, 1076–1084, May 2014.
14. Andújar, A. and J. Anguera, "MIMO multiband antenna system with non-resonant elements," *Microwave and Optical Technology Letters*, Vol. 57, No. 1, 183–190, Jan. 2015

15. Yang, C., Y. Yao, J. Yu, and X. Chen, "Novel compact multiband MIMO antenna for mobile terminal," *Int. J. Antennas Propag.*, Vol. 2012, 691681:1–691681:9, 2012.
16. Zeng, Q., Y. Yao, S. Liu, J. Yu, P. Xie, and X. Chen, "Tetra-band small size printed strip MIMO antenna for mobile handset application," *Int. J. Antennas Propag.*, Vol. 2012, 320582:1–320582:8, 2012.